Wuhan University
Journal of Natural Sciences

2023, Vol.28 No.4, 351-358

Article ID 1007-1202(2023)04-0351-08
DOI https://doi.org/10.1051/wujns/2023284351

Synthesis and Raman Performance Enhancement of Multilayer AuAg Heterostructures with Magnetic Resonance

HUANG Fan[1], ZHAO Zhirui[1], FENG Jingru[1], MA Liang[2†], DING Sijing[1†]

1. School of Mathematics and Physics, China University of Geosciences (Wuhan), Wuhan 430074, Hubei, China;

2. Hubei Key Laboratory of Optical Information and Pattern Recognition, Wuhan Institute of Technology, Wuhan 430205, Hubei, China

Abstract: Significant amplification of surface enhanced Raman scattering (SERS) signals can be achieved mainly by the electric field enhancement in metal core-shell nanostructures, and the enhanced magnetic field is rarely studied. In this study, we prepared multi-gap Au/AgAu core-shell hybrid nanostructures by using gold nanocup as the core. The overgrowth processes to grow one, two, and three layers of AgAu hybrid nanoshells can produce Au/AgAu[1], Au/AgAu[2], and Au/AgAu[3] heteronanostructures. The strong plasmon coupling between the core and shell leads to significant electromagnetic field enhancement. Under the synergistic effect of electromagnetic plasmon resonance and plasmon coupling, Au/AgAu core-shell hybrid nanostructures exhibit excellent SERS signals. We also investigate the effect of the interstitial position of the rhodamine B (RhB) molecule on Raman enhancement in Au/AgAu[3] heteronanostructures. This study can provide new ideas for the synthesis of multi-gap Raman signal amplifiers based on magnetic plasmon coupling.

Key words: Au/AgAu core-shell hybrid nanostructures; magnetic plasmon resonance; plasmon coupling; surface enhanced Raman scattering (SERS)

CLC number: O433.4

0 Introduction

Raman scattering effect refers to the effect that the frequency of light waves changes after being scattered. Through the analysis of Raman scattering spectrum, the relevant information of molecular vibration, rotation and structure can be obtained, which can be used to measure the content and concentration of the target substance qualitatively and quantitatively. The relevant detection methods are widely used in the fields of chemistry, biomedicine, environmental monitoring, food safety and so on[1-8]. However, in daily life, the Raman scattering signals of most substances are too weak to be tested, making it difficult and inaccurate to measure them using conventional methods. Therefore, people have been exploring methods that can enhance the Raman scattering signal of the tested substance[9-13]. Research has shown that

Received date: 2023-06-28
Foundation item: Supported by the National Natural Science Foundation of China (12274379, 11904332 and 11904270)
Biography: HUANG Fan, male, Undergraduate, research direction: micronano optics. E-mail: 201004169@cug.edu.cn
† To whom correspondence should be addressed. E-mail: maliang@wit.edu.cn; dingsijing@cug.edu.cn

Raman scattering intensity is enhanced to varying degrees when different molecules or ions are adsorbed on some metal surfaces, which is known as surface enhanced Raman scattering (SERS)[14-19].

At present, the research on SERS mainly focuses on the following three directions. First, precious metal nanoparticles are bonded together to form dimers, trimers, and even polymers, which is conducive to the formation of small gaps between nanoparticles to generate local field enhancement, so as to achieve SERS[20-24]. Second, nanostructures are prepared with rough surfaces, which have abundant and fully encircled hot spots due to the ultra-small nanogaps, sharp tips or non-uniform areas on the surface, thus achieving the effect of SERS[25-28]. Third, by multipling synthesis methods, core-shell nanostructures are prepared, and the gap between the shell layers is utilized to achieve the effect of SERS[29-34]. Li *et al*[35] synthesized a dimer of silver nanospheres without any additional assembly by optimizing the amount of chloride added to polyol synthesis to control the colloid stability and oxidation etching, and then studied the SERS effect of the hot spot of the dimer. Lin *et al*[36] synthesized a substrate modified with Au particles on ZnO nanorods using ion sputtering method, which had a very high Raman enhancement factor. This structure was expected to become an SERS substrate with high sensitivity and stability. Ding *et al*[37] prepared gold nanorods with adjustable surface roughness. The ultra-small nanogaps, sharp tips and non-uniform regions on the gold nanorods enabled them to have abundant and fully wrapped hot spots, and realized strong SERS. Hoeven *et al*[38] produced Au-Ag, Au-Pd and Au-Pt core-shell nanorods with precisely adjustable surface plasmon properties for adjustable SERS by performing metal overgrowth on gold nanorods within mesoporous silica shells. Tian *et al*[39] synthesized multi-layer shell core nanospheres (SiO_2@Au, SiO_2@Au@SiO_2) using liquid phase reduction method, and research has shown that the multi-layer nanospheres exhibit both cavity coupling and intra layer coupling, thereby improving local field enhancement and achieving high SERS performance. Ma *et al*[40] prepared two kinds of noble metal core-shell nanostars with different cores (Ag or Au) and the same Au shells with adjustable size and branch morphology, and studied their induced local surface plasmon resonance (LSPR) characteristics, and SERS performance.

According to the above knowledge, the enhancement of local field by the gap between core and shell is generally limited to the electric mode enhancement of isoplasmons, and there are few studies on the synergistic effect of magnetic resonance and gap to enhance local field[41-46]. In our previous work, we have studied the effect of magnetic resonance on local field in monolayer gap in detail[47]. In this work, we took the gold nanocup as the substrate and bonded rhodamine B (RhB) molecules in the first layer gap. Three kinds of core-shell nanostructures (Au/$AgAu^1$-RhB^1, Au/$AgAu^2$-RhB^1, and Au/$AgAu^3$-RhB^1) coated with single- , double- , and triple-layer AgAu hybrid nanoshells with gold nanocups as cores were prepared, and their Raman enhancement effects were tested. In order to study the enhancement effect of magnetic plasmon resonance and gap interaction on local fields of these structures further, the intermediate products were soaked in RhB aqueous solution at three different stages during the synthesis process. The three-gap Au/AgAu hybrid core-shell nanostructures (Au/$AgAu^3$-RhB^1, Au/$AgAu^3$-RhB^2, and Au/$AgAu^3$-RhB^3) of bonded Raman molecules in the first, second, and third interstitial gaps were obtained, respectively, and their Raman enhancement effects were tested under the same conditions.

1 Materials and Methods

1.1 Materials

Cetyltrimethylammonium bromide (CTAB, 99.0%) and cetyltrimethylammonium chloride (CTAC, 99.0%) were obtained from Aladdin. Thioacetamide (TAA, 99.0%), lead acetate ($Pb(Ac)_2$, 99.5%), ascorbic acid (AA, 99.7%), chloroauric acid ($HAuCl_4 \cdot 4H_2O$, 99.0%), silver nitrate ($AgNO_3$, 99.5%), hydrochloric acid (HCl, 36%-38%), Acetic acid (HAc, 99.5%) and rhodamine B ($C_{28}H_{31}ClN_2O_3$, 99.75%) were bought from Sinopharm Chemical Reagent Co. Ltd. (Shanghai, China). The solvents used in the experiment were all deionized water, with a resistivity of approximately 18.2 MΩ·cm.

1.2 Sample Preparation

We used the gold nanocup as the core, and prepared the core-shell nanostructures of gold nanocup core/silver gold hybrid nanoshell mediated by RhB using an adjustable electrical substitution and overgrowth process. The pre-prepared gold nanocup was mixed with RhB aqueous solution to make the outside of the gold nanocup absorb RhB molecule, and then growth solution prepared by silver nitrate was added to the gold nanocup solution

with RhB molecule adsorbed, so that a layer of silver shell grew on its surface. After the growth was completed, the above products were centrifuged and diluted with 2 mL of water, and then a growth solution prepared with chloroauric acid was added to it. The silver nanoshell was replaced with gold nanoshell using an electric replacement process to obtain the Au/$AgAu^1$-RhB^1 core-shell nanostructure. Repeat the above experimental operation and grow a layer of silver gold hybrid nanoshell on the periphery of the above product to obtain an Au/$AgAu^2$-RhB^1 core-shell nanostructure. Two layers of silver gold hybrid nanoshells were grown on the periphery of the above products to obtain Au/$AgAu^3$-RhB^1 core-shell nanostructures. The growth solution prepared by silver nitrate was dropped directly into the gold nanocup solution to make its surface grow a layer of silver shell. After centrifugation, the growth solution prepared by chloroauric acid was dropped into the product to obtain Au/$AgAu^1$ core-shell nanostructures. The product was mixed with RhB aqueous solution to make its surface absorb RhB molecules. Repeat the above experimental operation to grow two layers of silver gold hybrid nanoshells on its surface, then the Au/$AgAu^3$-RhB^2 core-shell nanostructure was obtained. The Au/$AgAu^2$ core-shell nanostructure was obtained by using the above process to grow two layers of silver gold hybrid nanoshell on the periphery of the gold nanocup. The product was mixed with RhB molecule, and then the silver gold hybrid nanoshell growing after the RhB molecule was adsorbed on its surface to obtain the Au/$AgAu^3$-RhB^3 core-shell nanostructure.

1.3 Characterization of Sample Characteristics

ATU-1810 UV-Vis spectrophotometer (China) was used to measure the extinction spectra of the sample. Scanning electron microscopy (SEM) was performed at 5.0 kV using Gemini 500 (Germany). Transmission electron microscopy (TEM) was performed at 200 kV using JEOL 2010 (Japan). Surface enhanced Raman scattering (SERS) spectra was acquired with the laser source with wavelength of 633 nm (1 mW) for 10 s of illumination on a HORIBA XploRA Plus Raman Microscope (France).

2 Results and Discussion

In order to study the SERS effect of different structures, we synthesized structures with different layers and different embedding positions of RhB, and measured their Raman enhancement effect. The schematic diagram of relevant structures is shown in Fig. 1.

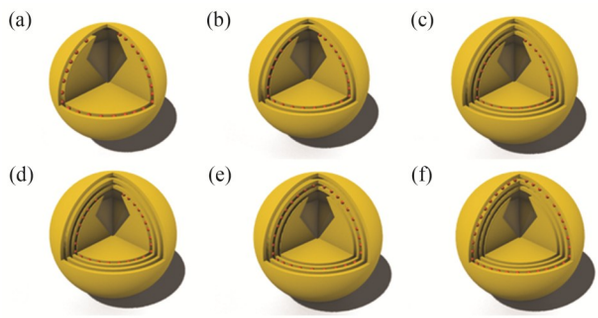

Fig. 1 Three-dimensional diagram of multilayer Au/AgAu core-shell nanostructure embedded by RhB

RhB molecules are embedded in the first layer gap of Au/AgAu core-shell nanostructures with (a) single-layer (Au/$AgAu^1$-RhB^1), (b) double-layer (Au/$AgAu^2$-RhB^1), and (c) triple-layer (Au/$AgAu^3$-RhB^1) Au/AgAu core-shell nanostructures. RhB molecules were embedded in different positions of the three-gap Au/AgAu core-shell nanostructure: (d) the first gap (Au/$AgAu^3$-RhB^1), (e) the second gap (Au/$AgAu^3$-RhB^2), and (f) the third gap (Au/$AgAu^3$-RhB^3)

Firstly, gold nanocups were obtained by selectively growing Au on PbS nanooctahedron and then dissolving PbS components. Using gold nanocups as starting substrate, Au/Ag core-shell nanostructures were synthesized by adding growth solution prepared by $AgNO_3$. Using it as a substrate, the growth solution configured by $HAuCl_4$ was added to the substrate, and the molar ratio of $HAuCl_4$ and $AgNO_3$ added to the growth solution was 1∶1. Au/$AgAu^1$ core-shell nanostructures were obtained through electrical substitution and overgrowth processes.

Figure 2(a) shows the SEM images of Au/$AgAu^1$ core-shell nanostructures. The gap between the gold nanocup core and the silver gold hybrid nanoshell can be clearly observed under a transmission electron microscope. These Au/AgAu core-shell nanostructures with gaps provide a good foundation for gap enhanced SERS based on magnetic plasmon coupling. By repeating the above process and controlling the molar ratio of $HAuCl_4$ and $AgNO_3$ added to each layer at 1∶1, Au/$AgAu^2$ core-shell nanostructures with two-layer gaps and Au/$AgAu^3$ core-shell nanostructures with three-layer gaps were synthesized. Figure 2(b) and (c) show the SEM images of Au/$AgAu^2$ and Au/$AgAu^3$ core-shell nanostructures, and Fig. 2(d)-(i) show the TEM images of the Au/$AgAu^1$, Au/$AgAu^2$ and Au/$AgAu^3$ core-shell nanostructures and their single particles, respectively. Under TEM, it can be observed that the Au/$AgAu^2$ core-shell nanostructure contains two layers of gaps, and the Au/$AgAu^3$ core-

shell nanostructure contains three layers of gaps. The width of the gaps decreases as it moves towards the outer layer. During the experiment, we also prepared the core-shell structure with notch, but the characterization results showed that the Raman enhancement effect of this structure was far worse than that of the circular core-shell structure, so the subsequent research focused on the circular core-shell structure.

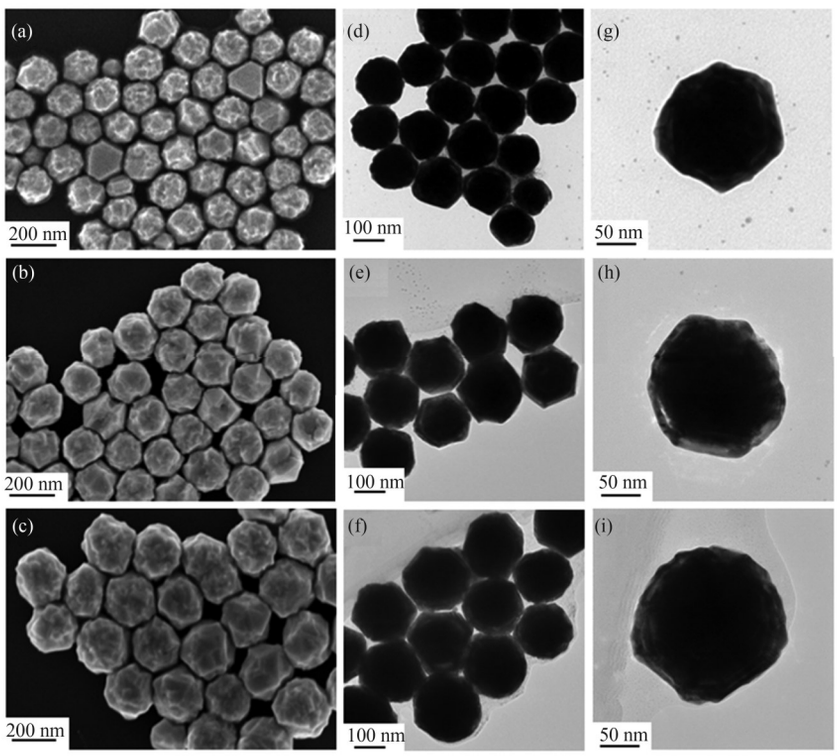

Fig. 2 SEM and TEM images of gold nanocup core/silver gold hybrid nanoshell structure and their single praticles
(a) SEM of Au/AgAu^{1}; (b) SEM of Au/AgAu^{2}; (c) SEM of Au/AgAu^{3}; (d) TEM of Au/AgAu^{1}; (e) TEM of Au/AgAu^{2}; (f) TEM of Au/AgAu^{3}; (g) TEM of Au/AgAu^{1} single particle; (h) TEM of Au/AgAu^{2} single particle; (i) TEM of Au/AgAu^{3} single particle

We used a visible ultraviolet spectrophotometer to determine the extinction spectra of the product, and studied the plasmon resonance properties of the gold nanocup/silver gold hybrid nanoshell core-shell nanostructure using extinction spectra. Figure 3(a) shows the extinction spectra of Au/AgAu^{1}-RhB^{1}, Au/AgAu^{2}-RhB^{1}, and Au/AgAu^{3}-RhB^{1} core-shell nanostructures at the same particle concentration. The plasmon resonance peak of the initial gold nanocup is located at 615 nm. After the gold nanocup was mixed with RhB aqueous solution, the growth solution containing $AgNO_3$ and the growth solution containing $HAuCl_4$ were added, then a layer of silver gold hybrid nanoshell was grown on the surface of the gold nanocup to obtain the Au/AgAu^{1}-RhB^{1} core-shell nanostructure. The above experimental operation was repeated and a layer of silver gold hybrid nanoshell was regenerated on the surface of the above product to obtain the Au/AgAu^{2}-RhB^{1} core-shell nanostructure. Continuing to repeat the operation, we obtained the product Au/AgAu^{3}-RhB^{1} with RhB molecule embedded in the first layer gap and three layers of AgAu hybrid nanoshells. Observing the extinction spectra of the three products, we found that with the increase of the number of AgAu hybrid nanoshells, the isoplasmon formant gradually redshifted, and the acromion appeared at 555 nm to the left of the main peak. With the increase of the number of shells, the acromion intensity gradually increased and produced a slight redshift. Figure 3(b) shows the extinction spectra of Au/AgAu^{3}-RhB^{1}, Au/AgAu^{3}-RhB^{2}, and Au/AgAu^{3}-RhB^{3} core-shell nanostructures at the same particle concentration. These three nanostructures are all wrapped with three layers of silver gold hybrid nanoshell on the surface of gold nanocup core. The difference is that RhB molecules are embedded in the first layer gap, the second layer gap and the third layer gap, respectively. The extinction spectrum shows that the plasmon resonance peaks of the three nanostructures are all located at 615 nm, and a shoulder

peak appears at 910 nm. With the embedding position of RhB molecular moving outward, the intensity of the shoulder peak gradually increases, accompanied by a slight red shift. During the process of couple replacement, a very narrow gap is formed between the shells, which can induce strong plasmon coupling and generate strong localized electromagnetic fields in the nanogap. These Au/AgAu^{1}, Au/AgAu^{2}, and Au/AgAu^{3} core-shell nanostructures provide reliable ideas for enhancing Raman signals.

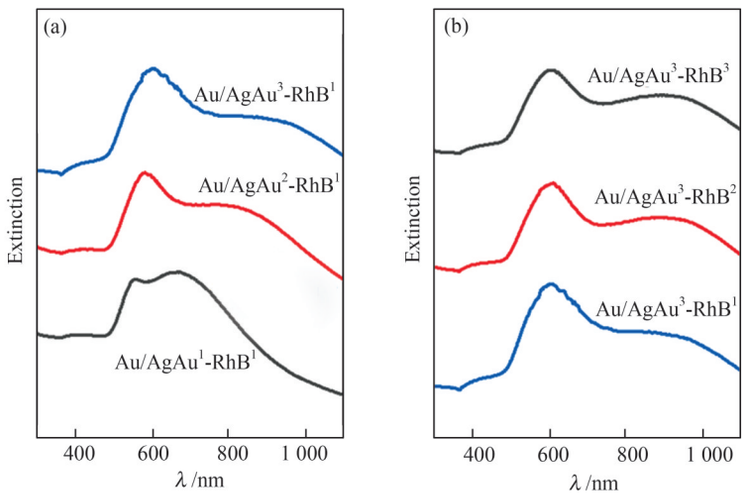

Fig. 3 Extinction spectra of Au/AgAu^{1}-RhB^{1}, Au/AgAu^{2}-RhB^{1}, Au/AgAu^{3}-RhB^{1} (a) and Au/AgAu^{3}-RhB^{1}, Au/AgAu^{3}-RhB^{2}, and Au/AgAu^{3}-RhB^{3} (b)

From the TEM images of the three products, the gaps between shell and core, as well as between shells, can be clearly observed. However, due to the denser shell, the observation effect on the gaps is not satisfactory. In order to display the internal structure of each product more clearly and intuitively, we took photos of the distribution of Au and Ag elements in the products of these three structures, as shown in Fig. 4. The content of gold in Au/AgAu^{1} core-shell nanostructures is much higher than that of silver, and the distribution is relatively uniform. Silver is mainly distributed on its surface, and there is a clear boundary for concentration changes in both distribution maps, which corresponds to the gaps in the nanostructure, as shown in Fig. 4(a). In the element distribution diagram of Au/AgAu^{2} core-shell nanostructures, two significant concentration changes can be observed, indicating the existence of two gaps in the structure, as shown in Fig. 4(b). In the element distribution map of Au/AgAu^{3} core-shell nanostructures, there are three significant concentration variation boundaries, indicating the existence of three gaps in the structure, and the lighter the color towards the outer side, the lower the element distribution concentration, and the smaller the width between the outer boundary and the boundary, indicating a smaller thickness towards the outer shell layer, as shown in Fig. 4(c).

Under the excitation of light with a wavelength of 633 nm, the SERS characteristics of gold nanocup core/silver gold nanoshell plasmon core shell nanostructures with RhB molecules embedded in the first layer gap and wrapped with one layer, two layers and three layers of silver gold shells were tested respectively. The measured results were in good agreement with the plasmon reso-

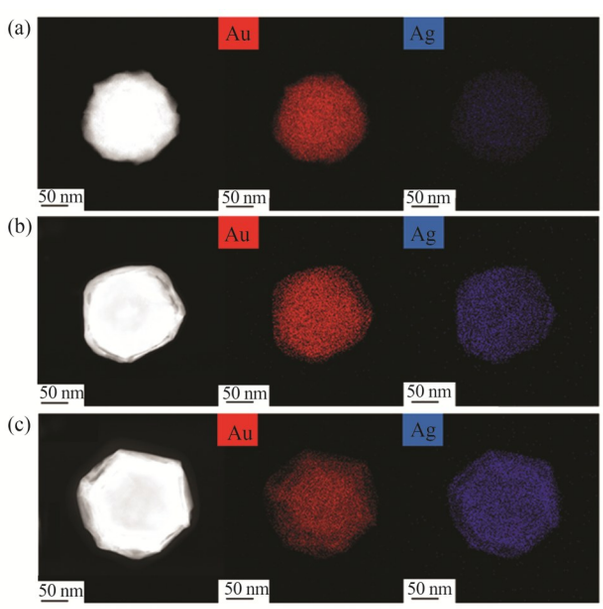

Fig. 4 Element distribution diagram of Au/AgAu^{1}(a), Au/AgAu^{2} (b) and Au/AgAu^{3} (c)

nance peak, as shown in Fig. 5(a). The Raman spectrum of RhB molecule is clearly visible, indicating that RhB molecule is well embedded in the nanogap. As the number of shell layers increases, the Raman intensity of this nanostructure sharply increases and rapidly decays. The Raman intensity of Au/AgAu^2-RhB^1 core-shell nanostructures is the strongest, and the peak broadening is the highest at around 1 500 nm. This is because there is only one-layer gap in the Au/AgAu^1-RhB^1 structure to enhance the Raman scattering signal, and the effect is poor. There is a double gap electromagnetic field coupling in the Au/AgAu^2-RhB^1 core-shell nanostructure, which has greatly enhanced the Raman scattering signal. However, the embedded position of RhB in the Au/AgAu^3-RhB^1 core-shell nanostructure is too deep, the outer shell is too thick, and the shielding effect on excitation is too strong, resulting in poor Raman scattering enhancement effect. Using the same method, we also measured the SERS characteristics of the gold nanocup core/silver gold nanoshell plasmon core shell nanostructure with RhB molecules embedded in the first layer, the second layer, and the third layer gaps, all wrapped with three layers of silver gold shells. The results are shown in Fig. 5(b). The structure showed that the Raman enhancement effect of RhB molecule was the weakest when it was connected to the first gap, and the Raman signal enhancement effect of RhB molecule when it was embedded into the second gap was much greater than that of the other two structures. This was due to the electromagnetic coupling between the first and third nanogaps in the three-gap nanostructure, which further enhanced the electromagnetic field in the second gap.

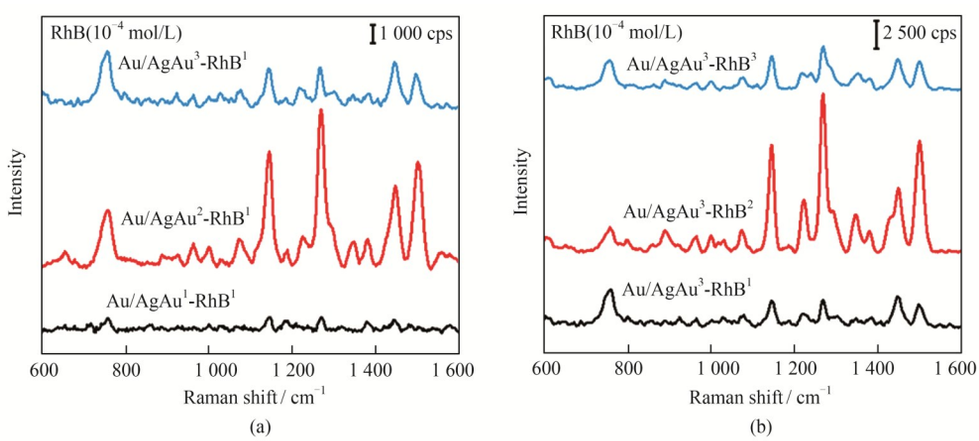

Fig. 5 Raman spectra of Au/AgAu^1-RhB^1, Au/AgAu^2-RhB^1, Au/AgAu^3-RhB^1(a) and Au/AgAu^3-RhB^1, Au/AgAu^3-RhB^2, and Au/AgAu^3-RhB^3(b)

3 Conclusion

In summary, we synthesized multilayered Au/AgAu core-shell nanostructures with RhB molecules embedded in the gaps, and studied the effects of the number of shells and the embedding position of RhB on the amplification of SERS signals. Au/AgAu hybrid nanostructures with adjustable number of gaps and RhB embedded position were synthesized by an adjustable electric substitution and surface overgrowth process based on gold nanocup. By immersing the initial Au nanocup or Au/AgAu hybrid in RhB aqueous solution, the selective binding of RhB molecules in the nanogap was achieved. Au/AgAu hybrid core-shell nanostructures exhibit significant plasmon absorption and electromagnetic field enhancement due to strong plasmon coupling in multi-nanogap structures, which makes Au/AgAu hybrid core-shell nanostructures have extremely strong SERS performance. And because the nanogaps between different shells interact with each other, and thus have different effects on the SERS effect, we embed RhB molecules to the surface of the gold nanocup directly, and grow one, two, and three layers of silver gold nanoshells on the outside, which are excited by the same light. The results show that the Au/AgAu hybrid core-shell nanostructures with two layers of nanogaps have the best SERS performance. This is because the coupling of double gap electromagnetic fields has a significant effect on the improvement of SERS performance. In addition, in order to obtain higher SERS performance, the position of RhB embedded in the Au/AgAu hybrid core-shell nanostructures with three-layer gaps was adjusted. The results

show that the three gap Au/AgAu hybrid core-shell nanostructures with RhB molecules embedded in the second nanogap exhibit the best SERS signal, due to the further enhancement of the electromagnetic field in the second layer gap, which is caused by the electromagnetic field coupling between the first layer and the third layer nanogap. Our research provides a new method for the synthesis of multi-gap Raman amplifiers based on magnetic isoplasmon coupling and has a wide range of applications in the preparation of Raman probes and sensitive detection in biomedical fields.

Conflicts of Interest

The authors declare no competing interests.

References

[1] Panneerselvam R, Liu G K, Wang Y H, *et al*. Surface-enhanced Raman spectroscopy: Bottlenecks and future directions[J]. *Chemical Communications*, 2018, **54**(1): 10-25.

[2] Alvarez-Puebla R A, Dos Santos D S Jr, Aroca R F. Surface-enhanced Raman scattering for ultrasensitive chemical analysis of 1 and 2-naphthalenethiols[J]. *Analyst*, 2004, **129**(12): 1251-1256.

[3] Pilot R, Signorini R, Durante C, *et al*. A review on surface-enhanced Raman scattering[J]. *Biosensors*, 2019, **9**(2): 57.

[4] Guerrini L, Krpetić Ž, van Lierop D, *et al*. Direct surface-enhanced Raman scattering analysis of DNA duplexes[J]. *Angewandte Chemie*, 2015, **127**(4): 1160-1164.

[5] Ong T T X, Blanch E W, Jones O A H. Surface enhanced Raman spectroscopy in environmental analysis, monitoring and assessment[J]. *Science of the Total Environment*, 2020, **720**: 137601.

[6] Jin H Z, Lu Q P, Chen X D, *et al*. The use of Raman spectroscopy in food processes: A review[J]. *Applied Spectroscopy Reviews*, 2016, **51**(1): 12-22.

[7] Inaba H, Kobayasi T. Laser-Raman radar—Laser-Raman scattering methods for remote detection and analysis of atmospheric pollution[J]. *Opto-Electronics*, 1972, **4**(2): 101-123.

[8] Hussain A, Sun D W, Pu H B. Bimetallic core shelled nanoparticles (Au@AgNPs) for rapid detection of thiram and dicyandiamide contaminants in liquid milk using SERS [J]. *Food Chemistry*, 2020, **317**: 126429.

[9] Kneipp K, Kneipp H, Itzkan I, *et al*. Surface-enhanced nonlinear Raman scattering at the single-molecule level[J]. *Chemical Physics*, 1999, **247**(1): 155-162.

[10] Wilson R, Bowden S A, Parnell J, *et al*. Signal enhancement of surface enhanced Raman scattering and surface enhanced resonance Raman scattering using *in situ* colloidal synthesis in microfluidics[J]. *Analytical Chemistry*, 2010, **82**(5): 2119-2123.

[11] Madzharova F, Heiner Z, Kneipp J. Surface enhanced hyper Raman scattering (SEHRS) and its applications[J]. *Chemical Society Reviews*, 2017, **46**(13): 3980-3999.

[12] Itoh T, Yoshida K, Biju V, *et al*. Second enhancement in surface-enhanced resonance Raman scattering revealed by an analysis of anti-Stokes and Stokes Raman spectra[J]. *Physical Review B*, 2007, **76**(8): 085405.

[13] Tolles W M, Nibler J W, McDonald J R, *et al*. A review of the theory and application of coherent anti-stokes Raman spectroscopy (CARS)[J]. *Applied Spectroscopy*, 1977, **31**(4): 253-271.

[14] Moskovits M. Surface roughness and the enhanced intensity of Raman scattering by molecules adsorbed on metals[J]. *The Journal of Chemical Physics*, 1978, **69**(9): 4159-4161.

[15] Wang D S, Kerker M. Enhanced Raman scattering by molecules adsorbed at the surface of colloidal spheroids [J]. *Physical Review B*, 1981, **24**: 1777-1790.

[16] Aiga N, Takeuchi S. Single-molecule Raman spectroscopy of a pentacene derivative adsorbed on the nonflat surface of a metallic tip[J]. *The Journal of Physical Chemistry C*, 2022, **126**(38): 16227-16235.

[17] Dutta Roy S, Ghosh M, Chowdhury J. Near-field response on the far-field wavelength-scanned surface-enhanced Raman spectroscopic study of methylene blue adsorbed on gold nanocolloidal particles[J]. *The Journal of Physical Chemistry C*, 2018, **122**(20): 10981-10991.

[18] Marques F C, Oliveira G P, Teixeira R A R, *et al*. Characterization of 11-mercaptoundecanoic and 3-mercaptopropionic acids adsorbed on silver by surface-enhanced Raman scattering[J]. *Vibrational Spectroscopy*, 2018, **98**: 139-144.

[19] Nikoobakht B, Wang J P, El-Sayed M A. Surface-enhanced Raman scattering of molecules adsorbed on gold nanorods: Off-surface plasmon resonance condition[J]. *Chemical Physics Letters*, 2002, **366**(1/2): 17-23.

[20] Kumar J, Thomas K G. Surface-enhanced Raman spectroscopy: Investigations at the nanorod edges and dimer junctions[J]. *The Journal of Physical Chemistry Letters*, 2011, **2** (6): 610-615.

[21] Talley C E, Jackson J B, Oubre C, *et al*. Surface-enhanced Raman scattering from individual Au nanoparticles and nanoparticle dimer substrates[J]. *Nano Letters*, 2005, **5**(8): 1569-1574.

[22] Chirumamilla M, Toma A, Gopalakrishnan A, *et al*. 3D nanostar dimers with a sub-10-nm gap for single-/ few-molecule surface-enhanced Raman scattering[J]. *Advanced Materials*,

2014, **26**(15): 2353-2358.

[23] Kang H S, Zhao W Q, Zhou T, *et al*. Toroidal dipole-modulated dipole-dipole double-resonance in colloidal gold rod-cup nanocrystals for improved SERS and second-harmonic generation[J]. *Nano Research*, 2022, **15**(10): 9461-9469.

[24] Wustholz K L, Henry A I, McMahon J M, *et al*. Structure–activity relationships in gold nanoparticle dimers and trimers for surface-enhanced Raman spectroscopy[J]. *Journal of the American Chemical Society*, 2010, **132**(31): 10903-10910.

[25] Luo Y, Aubry A, Pendry J B. Electromagnetic contribution to surface-enhanced Raman scattering from rough metal surfaces: A transformation optics approach[J]. *Physical Review B*, 2011, **83**(15): 155422.

[26] Khlebtsov B, Khlebtsov N. Surface-enhanced Raman scattering-based lateral-flow immunoassay[J]. *Nanomaterials*, 2020, **10**(11): 2228.

[27] Lin M H, Sun L, Kong F B, *et al*. Rapid detection of paraquat residues in green tea using surface-enhanced Raman spectroscopy (SERS) coupled with gold nanostars[J]. *Food Control*, 2021, **130**: 108280.

[28] Nalbant Esenturk E, Hight Walker A R. Surface-enhanced Raman scattering spectroscopy via gold nanostars[J]. *Journal of Raman Spectroscopy*, 2009, **40**(1): 86-91.

[29] Shirzaditabar F, Saliminasab M, Arghavani Nia B. Triple plasmon resonance of bimetal nanoshell[J]. *Physics of Plasmas*, 2014, **21**(7): 072102.

[30] He Z, Zhu J, Li X, *et al*. Surface etching-dependent geometry tailoring and multi-spectral information of Au@AuAg yolk-shell nanostructure with asymmetrical pyramidal core: The application in Co^{2+} determination[J]. *Journal of Colloid and Interface Science*, 2022, **625**: 340-353.

[31] Liu P, Chen H J, Wang H, *et al*. Fabrication of Si/Au core/shell nanoplasmonic structures with ultrasensitive surface-enhanced Raman scattering for monolayer molecule detection[J]. *The Journal of Physical Chemistry C*, 2015, **119**(2): 1234-1246.

[32] Dai L W, Song L P, Huang Y J, *et al*. Bimetallic Au/Ag core-shell superstructures with tunable surface plasmon resonance in the near-infrared region and high performance surface-enhanced Raman scattering[J]. *Langmuir*, 2017, **33** (22): 5378-5384.

[33] Ma L A, Chen Y L, Yang D J, *et al*. Gap-dependent plasmon coupling in Au/AgAu hybrids for improved SERS performance[J]. *The Journal of Physical Chemistry C*, 2020, **124** (46): 25473-25479.

[34] Yilmaz A, Yilmaz M. Bimetallic core–shell nanoparticles of gold and silver via bioinspired polydopamine layer as surface-enhanced Raman spectroscopy (SERS) platform[J]. *Nanomaterials*, 2020, **10**(4): 688.

[35] Li W Y, Camargo P H C, Lu X M, *et al*. Dimers of silver nanospheres: Facile synthesis and their use as hot spots for surface-enhanced Raman scattering[J]. *Nano Letters*, 2009, **9** (1): 485-490.

[36] Lin Y, Zhang J, Zhang Y L, *et al*. Multi-effect enhanced Raman scattering based on Au/ZnO nanorods structures[J]. *Nanomaterials*, 2022, **12**(21): 3785.

[37] Ding S J, Ma L, Feng J R, *et al*. Surface-roughness-adjustable Au nanorods with strong plasmon absorption and abundant hotspots for improved SERS and photothermal performances[J]. *Nano Research*, 2022, **15**(3): 2715-2721.

[38] van der Hoeven J E S, Deng T S, Albrecht W, *et al*. Structural control over bimetallic core-shell nanorods for surface-enhanced Raman spectroscopy[J]. *ACS Omega*, 2021, **6**(10): 7034-7046.

[39] Tian W H, Wu K Y, Cheng X L, *et al*. Preparation and analysis of the Au-SiO_2 multi-layer nanospheres as high SERS resolution substrate[C]//*Optical Sensors and Biophotonics*. Washington D C: Optica Publishing Group, 2011: 83110K.

[40] Ma J M, Liu X F, Wang R W, *et al*. Bimetallic core-shell nanostars with tunable surface plasmon resonance for surface-enhanced Raman scattering[J]. *ACS Applied Nano Materials*, 2020, **3**(11): 10885-10894.

[41] Metiu H. Surface enhanced spectroscopy[J]. *Progress in Surface Science*, 1984, **17**(3/4): 153-320.

[42] Tsang J C, Kirtley J R, Bradley J A. Surface-enhanced Raman spectroscopy and surface plasmons[J]. *Physical Review Letters*, 1979, **43**(11): 772-775.

[43] Hamon C, Liz-Marzán L M. Colloidal design of plasmonic sensors based on surface enhanced Raman scattering[J]. *Journal of Colloid and Interface Science*, 2018, **512**: 834-843.

[44] Alvarez-Puebla R A, Ross D J, Nazri G A, *et al*. Surface-enhanced Raman scattering on nanoshells with tunable surface plasmon resonance[J]. *Langmuir*, 2005, **21**(23): 10504-10508.

[45] Chen S Q, Han L, Schülzgen A, *et al*. Local electric field enhancement and polarization effects in a surface-enhanced Raman scattering fiber sensor with chessboard nanostructure [J]. *Optics Express*, 2008, **16**(17): 13016.

[46] Lee J, Hua B, Park S, *et al*. Tailoring surface plasmons of high-density gold nanostar assemblies on metal films for surface-enhanced Raman spectroscopy[J]. *Nanoscale*, 2014, **6**(1): 616-623.

[47] Zhao Z R, Zhang S, Jing R P, *et al*. Synthesis of magnetic plasmonic Au/AgAu heterostructures with tunable gap width for enhancing Raman performance[J]. *Plasmonics*, 2023, **18**: 283-289.

□